Ocean Systems Engineering, *Vol. 7, No. 3 (2017) 179-193*
DOI: https:// doi.org/10.12989/ose.2017.7.3.179

Nonlinear response of stiffened triceratops under impact and non-impact waves

Srinivasan Chandrasekaran* and Jamshed Nassery[a]

Department of Ocean Engineering, Indian Institute of Technology Madras, India

(Received May 28, 2017, Revised August 20, 2017, Accepted August 26, 2017)

Abstract. Dynamic response analysis of offshore triceratops with stiffened buoyant legs under impact and non-impact waves is presented. Triceratops is relatively new-generation complaint platform being explored in the recent past for its suitability in ultra-deep waters. Buoyant legs support the deck through ball joints, which partially isolate the deck by not transferring rotation from legs to the deck. Buoyant legs are interconnected using equally spaced stiffeners, inducing more integral action in dispersing the encountered wave loads. Two typical nonlinear waves under very high sea state are used to simulate impact and non-impact waves. Parameters of JONSWAP spectrum are chosen to produce waves with high vertical and horizontal asymmetries. Impact waves are simulated by steep, front asymmetric waves while non-impact waves are simulated using Stokes nonlinear irregular waves. Based on the numerical analyses presented, it is seen that the platform experiences both steady state (springing) and transient response (ringing) of high amplitudes. Response of the deck shows significant reduction in rotational degrees-of-freedom due to isolation offered by ball joints. Weak-asymmetric waves, resulting in non-impact waves cause steady state response. Beat phenomenon is noticed in almost all degrees-of-freedom but values in sway, roll and yaw are considerably low as angle of incidence is zero degrees. Impact waves cause response in higher frequencies; bursting nature of pitch response is a clear manifestation of the effect of impact waves on buoyant legs. Non-impact waves cause response similar to that of a beating phenomenon in all active degrees-of-freedom, which otherwise would not be present under normal loading. Power spectral density plots show energy content of response for a wide bandwidth of frequencies, indicating an alarming behaviour apart from being highly nonlinear. Heave, being one of the stiff degrees-of-freedom is triggered under non-impact waves, which resulted in tether tension variation under non-impact waves as well. Reduced deck response aids functional requirements of triceratops even under impact and non-impact waves. Stiffened group of buoyant legs enable a monolithic behaviour, enhancing stiffness in vertical plane.

Keywords: asymmetrical wave; ball joint; impact; non-impact; stiffened offshore triceratops; tether tension variation; buoyant legs

1. Introduction

Complexities in deep water oil exploration demand an adaptable structural form, which could alleviate lateral loads without compromising complaint characteristics that are advantageous and

*Corresponding author, Professor, E-mail: drsekaran@iitm.ac.in
[a] Institute Post-doctoral fellow, Email: jamshednc@gmail.com

http://www.techno-press.org/?journal=ose&subpage=7 ISSN: 2093-6702 (Print), 2093-677X (Online)

cost effective (Chandrasekaran, 2016, 2015a, b). Steep and large amplitude waves produce nonlinear motion and dynamic tether tension variations in offshore compliant structures (Chandrasekaran *et al.* 2011, 2010b). While they remain positive buoyant and permitted to undergo large displacements in horizontal plane (surge and sway motion), vibrations caused by the impact waves (ringing) and non-impact waves (springing) at high frequencies are vital (Chandrasekaran and Jain 2016); they could result in responses of undesirable amplitudes (Chandrasekaran *et al*. 2010a). Several researchers examined response behaviour of innovative structural forms of offshore platforms to assess their adaptability to deep waters (Chandrasekaran 2014, Halkyard 1991, Jeffreys and Rainey 1994, Murert *et al.* 1996, Tromans *et al.* 2006). While current codes accommodate such effects in the design of compliant structures like Tension Leg Platforms (TLP), detailed studies on stiffened triceratops is scarce in the literature. Offshore triceratops is a recent development, which effectively counteracts the lateral loads by its innovative geometric form (White *et al*. 2005, Shaver *et al*. 2011, Chaplin *et al*. 1993, Chandasekaran and Madhuri Nannaware 2013, Capanoglu *et al*. 2002).

Triceratops consists of a deck, supported by three set of buoyant legs, which are taut-moored to the seabed. Ball joints, placed between the deck and the buoyant legs restrain transfer of rotational displacements from the legs to the deck and vice-versa (Chandrasekaran *et al*. 2013, 2010c, Chandrasekaran and Madhuri 2012a, b). By inter-connecting the buoyant legs using stiffeners, stiffness of the platform in horizontal plane shall be enhanced (Chandrasekaran and Mayank 2017, Chandrasekaran and Madhuri 2015, 2012). Fig. 1 shows the conceptual view of different components of the stiffened triceratops. Weight of topside, ballast and pretension in the restoring system are counteracted by virtue of the excess buoyancy. Under environmental loads, most of the complaint offshore structures show increase in stresses due to rigid connections. On the other hand, triceratops counter act them by virtue of its structural form. Top deck rests on buoyant legs; ball joints placed in between them allow transfer of translation and restrain rotation between them. Ball joints reduce undesirable responses of the deck even for a larger response of the buoyant legs. Triceratops remain flexible in horizontal plane resembling a TLP; stiff in vertical plane due to deep-draft buoyant legs, resembling a spar. Presence of articulated joints could be one of the most suitable structural forms of offshore platforms for deep waters (Chandrasekaran *et al*. 2010a, 2006); salient advantages when deployed in articulated loading platforms, processing platforms and multi-leg articulated towers are established well through experimental and numerical studies.

2. Impact and non-impact waves

Ocean waves are mathematically modeled as linear, weakly nonlinear and highly or strongly nonlinear (Longuet and Cokelet 1976). Linear wave is symmetric about both the axes whereas nonlinear waves are generally asymmetric about the horizontal and vertical axes through crests and troughs (Tucker *et al.* 1984, Chandrasekaran *et al.* 2011). Strongly asymmetric wave simulates impact wave and weakly nonlinear or asymmetric wave generates non- impact wave (Kim *et al.* 1998). Impact force is caused by collision of upright wave front with the structure. This leads to a change in the forward momentum, which yields a force of larger magnitude of a short duration. Response of the member under the maximum impact force is governed by its dynamic characteristics. Rising time, at which the impact force reaches its maximum amplitude, is vital. Angle of the inclined wave front also governs the rising time and rise in amplitude of impact force. Impact waves have a distinct convex front and concave rear with a strong asymmetry about both horizontal and vertical axes (Kim *et al*. 1997). Vertical asymmetry is expressed by the ratio of falling to rising period of the

crest, field data of which varies from 1.2 to 2.1 (Myrhaug and Kjeldsen 1984). All other waves, which do not possess the above property are considered as weak-asymmetric. Amongst the Gaussian (linear) time series of wave elevation comprising large wave groups, largest wave group is deformed to become strong asymmetric waves. Complex amplitude spectrum, which is necessary to generate strong asymmetric wave can be simulated using FFT tools (Kim *et al*. 1992). Major contribution to transient response arise from the steep-front asymmetric, energetic waves (Zou and Kim 2000). Dynamic nonlinear response of the platform is investigated under these impact and non-impact loads. Offshore triceratops, when subjected to strong asymmetric and weakly nonlinear waves is likely to exhibit transient (ringing) and steady state responses (springing), which are of larger interest.

Response under impact waves involves analyses of transient structural deflections at (or closer to) natural frequency of the platform, which arise at third-harmonic of the incident wave field. Non-impact waves induce excitation in the vertical plane, even though it is stiff. Several researchers successfully simulated impact and non-impact using predefined spectrum (Tromans *et al*. 2006). Range of significant wave height specifies the sea states or sea severity is shown in Table 1 (Price and Bishop, 1974). For the North Sea environment, a storm sea state, defined by peak period and significant wave height is used in the present study. For transient response, dominant wave frequency is assumed to be several times higher than that of the surge natural frequency of the platform. In the present study, JONSWAP spectrum is used to simulate asymmetric waves using the following equations (Isherwood 1987)

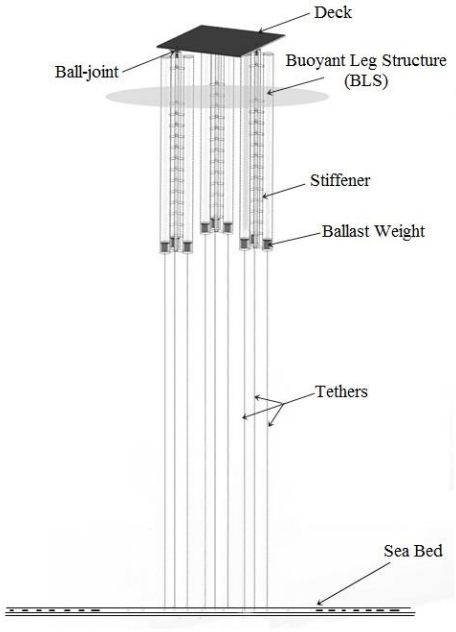

(a) Elevation

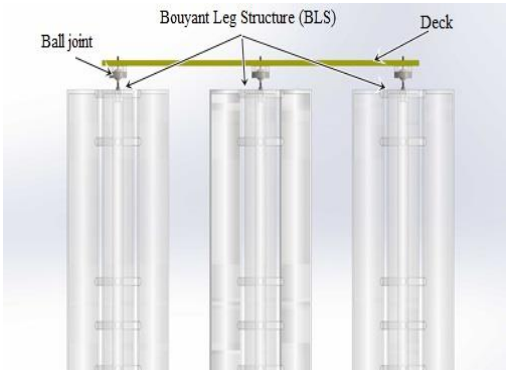

(b) Stiffeners

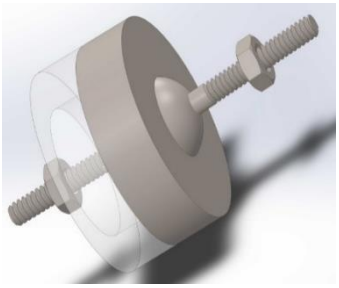

(c) Ball joint

Fig. 1 Conceptual view of stiffened triceratops

Table 1 Description of sea state

Code	Description of sea state	Significant wave height (m)
0	Calm (glassy)	0
1	Calm (rippled)	0.0 to 0.1
2	Smooth (wavelets)	0.1 to 0.5
3	Slight	0.5 to 1.25
4	Moderate	1.25 to 2.5
5	Rough	2.5 to 4
6	Very rough	4 to 6
7	High	6 to 9
8	Very high	9 to 14
9	Phenomenal	Over 14

$$S_{\eta\eta}(f)=\alpha g^2(2\pi)^{-4} f^{-4} \exp\left[-1.25\left(\frac{f}{f_m}\right)^{-4}\right]\gamma^{\exp\left[\frac{(f-f_m)^2}{2\sigma^2 f_m^2}\right]} \tag{1}$$

$$\begin{aligned}\sigma &= \sigma_a = 0.07\{\text{for } f \le f_m\}\\ \sigma &= \sigma_b = 0.09\{\text{for } f > f_m\}\end{aligned} \tag{2}$$

where, f is frequency (in Hz); f_m is the frequency corresponding to maximum $S_{\eta\eta}(f)$ for generating an impact wave. Wave steepness (s) is given by

$$s = \frac{2\pi H}{gT_z^2} \tag{3}$$

$$\gamma = 10.54\text{-}1.34s^{-1/2} - \exp\{-19+3.775s^{-1/2}\} \text{ for } s > 0.037 \tag{4}$$

$$\gamma = 0.9+\exp\{18.86-3.67s^{-1/2}\} \text{ for } s < 0.037 \tag{5}$$

Philips constant (α) can be determined from the following relationship

$$\frac{\alpha}{s^2} = 2.964+0.4788\sqrt{\gamma}-0.343\gamma+0.04225\sqrt[3/4]{\gamma} \tag{6}$$

3. Numerical analyses

Conceptual model of different components of the platform is given in Fig. 1. Numerical modeling of the platform is carried out in ANSYS AQWA workbench. As buoyant legs qualify for the Morison region, each leg is modeled as tube elements with segments spread along its length; deck is modeled

as quadrilateral plate elements. As components of the platform are independent in their structural properties (mass, radius of gyration and center of gravity), each unit is modeled as a separate entity. Hydro- static and free-floating characteristics of the platform are obtained from the Design Modeler. Pretension in tethers, including its self-weight is computed in Librium analysis, which checks the equilibrium of each unit and the complete platform as well. As wave forces are time-variant, implicit nonlinearity is resulted from the change in buoyancy at every step. This results in dynamic tether tension variations, which are also nonlinear functions of platform motion. Coefficients of the stiffness matrix are influenced by the change in pretension in each tether, which updates the lateral and longitudinal stiffness of the platform. Variable buoyancy also affects the added mass of platform, which in turn updates the inertia force. Since the relative, square drag and inertia forces are nonlinear, response of the platform also becomes nonlinear. Tethers are modeled as flexible members using their cross sectional area, length, density and modulus of elasticity of the material. As the chosen software does not consider the mass of fluid in the flooded cylinder, added mass in surge and sway degrees-of-freedom is considered as an additional input for the analysis to include the moon-pool effect. Equation of motion is solved by considering nonlinear stiffness matrix, which is updated at every time step of solution; response of the structure is obtained at center of mass of the deck.

Nonlinear time history analyses using numerical technique are carried out in ANSYS AQWA Naut module by considering variations in submergence effect, stiffness, buoyancy, inertia and nonlinear drag forces. By considering radius of the buoyant leg equals to that of the hemisphere, hemispherical fluid mass of each buoyant leg unit is considered as the heave added mass in the analysis. Two sea states namely: very high and high (please refer Table 1 for details) with a significant wave height of 9.88 m and 7.62 m are chosen to simulate impact and non-impact waves. Table 2 shows details of different wave set with varying peakness parameters and vertical asymmetry factors, used to simulate impact and non-impact waves. Parameters of JONSWAP spectrum (Hs = 9.88 m, T_z = 11.02 s, γ = 6.5, vertical asymmetry = 2.15) produces a strongly asymmetric wave, designated as wave A. As wave A possess high vertical asymmetric parameter, this wave is similar to that of impact waves, causing ringing phenomenon. Other set of wave, designated as wave E has parameters (Hs = 7.62 m, T_z = 12.65 s, γ = 3.0, vertical asymmetry = 0.63) is capable of simulating non-impact waves, causing springing phenomenon.

Table 2 Details of different wave set

Wave set	H_S(m)	T_Z (s)	Peakness parameter (γ)	Vertical asymmetry factor	Skewness	Kurtosis
A	9.88	11.02	6.5	2.15	0.28	3.15
B	10.77	13.60	2.5	0.79	0.01	----
C	10.80	14.10	2.0	0.53	-0.07	2.85
D	15.40	17.80	1.7	1.52	----	----
E	7.62	12.65	3.0	0.63	0.12	2.82

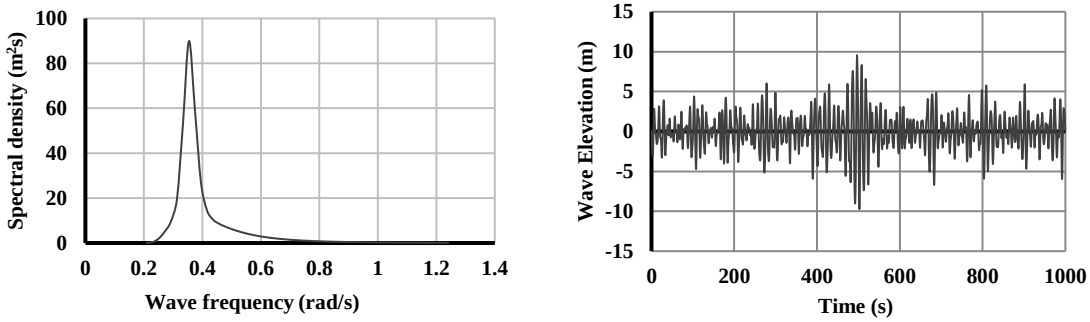

(a) (b)

Fig. 2 (a) Spectrum of wave A and (b) Profile of impact wave A

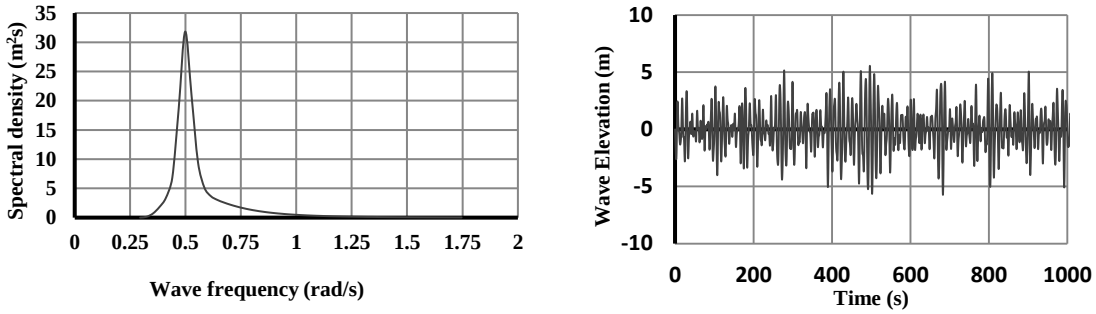

(a) (b)

Fig. 3 (a) Spectrum of wave E and (b) Profile of non-impact wave E

It is seen from Table 2 that asymmetry increases with the increase in significant wave height, while decreases significantly with the increase in the zero-crossing period. Wave A is strongly asymmetric while wave E is weakly asymmetric. Wave elevations of A and E irregular waves are generated numerically as shown in Figs. 2 and 3, respectively. It is seen from the figures that Wave A is irregular with finite repeating periods and contains a strong asymmetric wave near 495s; such waves create impact effects on the encountered structures. Alternatively, wave E has large randomness and capable of causing non-impact effects (Zou and Kim 2000). While skewness is a measure of wave asymmetry about horizontal axis, wave A is strongly asymmetric. Skewness of wave B is closer to zero and hence unable to produce strong asymmetric waves.

4. Response under impact waves

Details of the platform considered for the study are given in Table 3. In the numerical analysis, responses of a typical group of buoyant leg and the deck are evaluated separately. Variations in the

responses between the groups of buoyant leg are not significant, as all the three groups of buoyant legs share the encountered load proportionally. Hydrodynamic interaction between the groups of buoyant legs is not focused; response of buoyant leg is considered as a single unit as stiffeners integrally connect each group. Fig. 5 shows the response time history and power spectral density of a typical buoyant leg group under impact waves in different degrees-of-freedom; sway and roll responses are not significant and hence not plotted. It is seen from the figures that impact waves cause response in higher frequencies in all active degrees-of-freedom, which otherwise would be present due to coupling between the degrees-of-freedom.

Triceratops inherits stiffness from deep-draft of buoyant leg and taut-moored tethers. PSD of heave shows one significant peak at about 0.38 Hz (= 2.63s). This is occurring closer to the vicinity of heave period and its coupling with that of pitch, as heave and pitch periods are 4.8s and 3.42s, respectively.

Table 3 Structural properties of stiffened triceratops

Description	Value
Water depth	600 m
Material	Steel
Unit weight of the material	7850 kg/m^3
Centre to centre distance of the legs	70 m
Diameter of each leg (moon pool + individual leg)	12.9 m (= 8.4 + 4.5)
Free board	22 m
Draft	74.7 m
Length of each leg	96.7 m
Tether length	525.3 m
Unit weight of surrounding fluid	1025 kg/m^3
Buoyancy	300210 kN
Area of deck	1732.41 m^2
Self weight + payload	296.45 MN
Radius of gyration of buoyant leg (r_{xx}, r_{yy})	33.31 m
Radius of gyration of deck (r_{xx}, r_{yy})	24.9 m
Axial stiffness of tether	84.0E+03 kN/m
Cross-sectional area of tethers in each group of buoyant leg	0.22 m^2
Natural period in surge/ sway	88.4 s/ 96 s
Natural period in heave	2.8 s
Natural period in roll, pitch	3.42 s

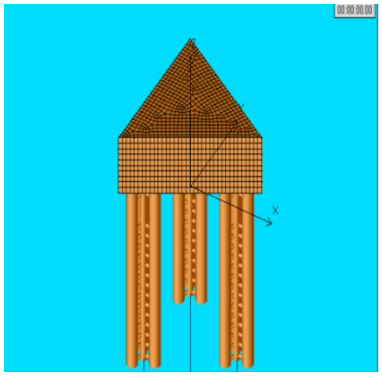

(a) Stiffened triceratops

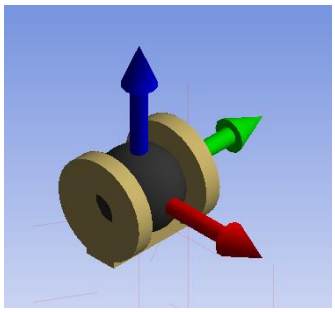

(b) Ball joint

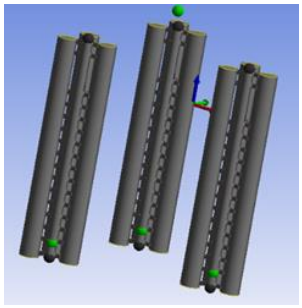

(c) Stiffened buoyant leg group

Fig. 4 Numerical model of stiffened triceratops

Successive peaks occurring at higher frequencies of 0.9 Hz and 1.8 Hz shall be attributed to increased stiffness behaviour caused by stiffeners, which interconnect the buoyant legs. As each leg is not free to rotate about the ball joint, it signifies a stiff behaviour. In addition, restraint caused to free rotation of ball joints, due to large number of cycles of response shall also be responsible for this high-frequency response. This is more clear in the pitch response. First and the smallest peak seen in PSD of pitch response, which is appearing closer to zero is attributed to the coupling effect of surge and pitch degrees-of-freedom; surge frequency is at 0.01 Hz. Successive peak appears at 0.1 Hz, which is closer to the wave frequency of Wave set A, which is an impact wave. Next peak, appearing at 0.2 Hz arise due to the differential heave caused by pitch motion. Differential heave is caused by tension variation in tethers; it is not same in all buoyant legs. This influences pitch response (or roll, as the case may be). A larger peak, appearing at higher frequency is a celar manifestation of stiffness induced to the system by both stiffeners that interconnect the buoyant legs and restraint of rotation to ball joints, caused by large number of cycles of response. It is important to note that the bursting nature of pitch response, occurring closer to 495s is a clear manifestation of the effect of impact waves on buoyant legs. Yaw response, which is quite unusual under uni-directional waves on a symmetric platform is due to the resultant of pitch and surge responses; magnitude of this is insignificant. Other nonlinearities that arise from differential heave settlement, variable submergence (high draft+large pretension), response coupling between different degrees-of-freedom are responsible for the shift in maximum amplitude in pitch response that of its natural frequency.

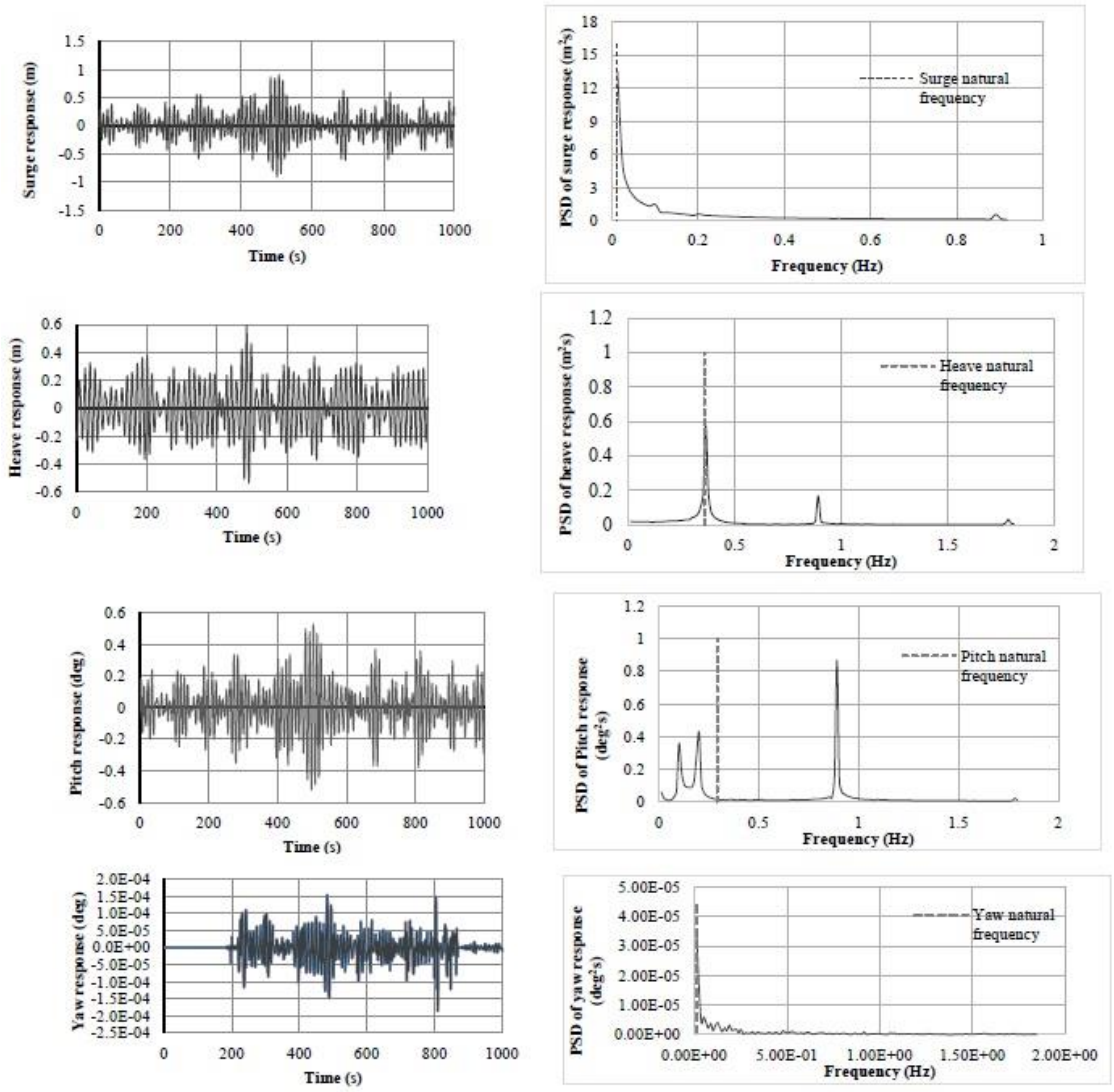

Fig. 5 Response of a buoyant leg group under impact waves (Wave set A)

As triceratops remain stiff in vertical plane due to taut-moored system, impact waves also cause dynamic tether tension variations, as shown in Fig. 6. It is seen from the figure that tension variation is maximum at 500s but pitch response is not maximum at this time instant. Maximum tension variation is resulting from variable submergence effect due to impact load on the stiffened triceratops and nonlinear effect of waves; asymmetricity of the wave is maximum at this point. Further, there is a strong coupling between pitch and differential heave, caused by tension variation. It is also

observed that the variations in the maximum amplitude of tether tension is about 2.5% of that of the initial pretension. It is therefore important to note that tether pull-out, causing instability to the platform may not occur under this marginal variation but cause burst like responses are caused in pitch degree-of-freedom. This may challenge safe operability of the platform; but, thanks to the presence of ball joints, rotational responses are not transferred from the legs to the deck, as seen from Fig. 7. Statistical analysis of tether tension variation is important to confirm the fact that it is resulted from impact waves. Maximum amplitude more than seven times of that of the standard deviation and coefficient of kurtosis exceeding five shall be seen as consequences of impact wave response (Jeffreys and Rainey 1994, Halkyard *et al*. 1991). Table 4 shows the statistical values of tether tension variation under both wave sets, A and E respectively. By observation, it is evident that tether tension variations caused by wave set A are due to impact waves.

Table 4 Statistics of tether tension variation

Description	Wave set A	Wave set E
Mean (N)	1.3×10^6	1.28×10^6
Variance (N^2)	1.84×10^{10}	1.32×10^{10}
Standard Deviation (N)	1.36×10^5	1.15×10^5
Skewness	0.28	0.14
Kurtosis	5.75	2.63

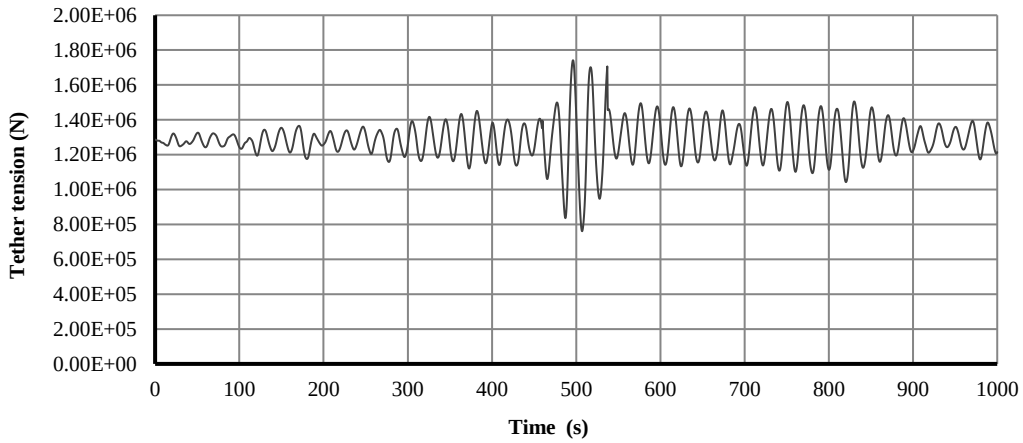

Fig. 6 Dynamic tether tension variations under impact waves (wave set A)

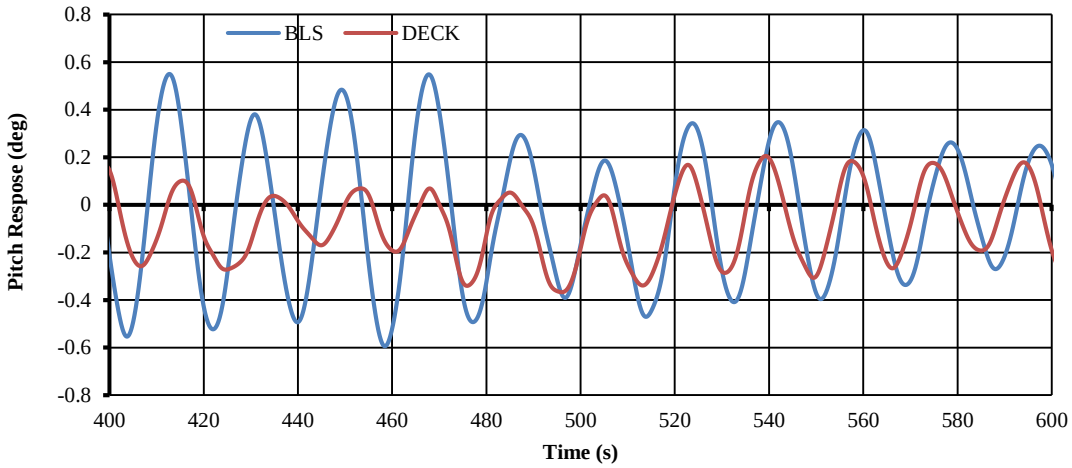

Fig. 7 Comparison of pitch responses under impact waves (wave set A)

5. Response under non-impact waves

Wave set E is classified as non-impact waves. Wave E has parameters (Hs = 7.62 m, T_z = 12.65 s, γ = 3.0, vertical asymmetry = 0.63) that are capable of simulating non-impact waves, causing springing phenomenon. Fig. 8 shows the response time history and power spectral density of a typical buoyant leg group under non-impact waves in different degrees-of-freedom. It is seen from the figures that non-impact waves cause response similar to that of a beating phenomenon in all active degrees-of-freedom, which otherwise would not be present under normal loading. Power spectral density plots show energy content of response for a wide bandwidth of frequencies, indicating an alarming behaviour, apart from being highly nonlinear. Heave, being one of the stiff degrees-of-freedom is triggered under non-impact waves, which prompts to examine the probability of tendon failure.

Non-impact waves also cause dynamic tether tension variations, as shown in Fig. 9. It is seen that the variations in the maximum amplitude of tether tension is about 2.2% of that of the initial pretension. Even though this may not result in tendon failure, but springing response of buoyant legs may affect the deck response; but, thanks to the presence of ball joints, rotational responses are not completely transferred from the legs to the deck, as seen from Fig. 10. However, it is important to note that springing response affects the deck in significant proportion in comparison to that of the ringing response (Please see Fig. 7 for minimum deck response under impact waves). Statistical analysis of tether tension variation is important to confirm the fact that it is resulted from non-impact waves. Table 4 shows the statistical values of tether tension variation under wave E. It is seen that coefficient of Kurtosis of tether tension variations is 2.82, which is lesser than five; further, maximum amplitude of tether tension variation, caused by wave set E is about 5.7 times of that of the standard deviation. Above figures verify that these are consequences of non-impact waves on tether response.

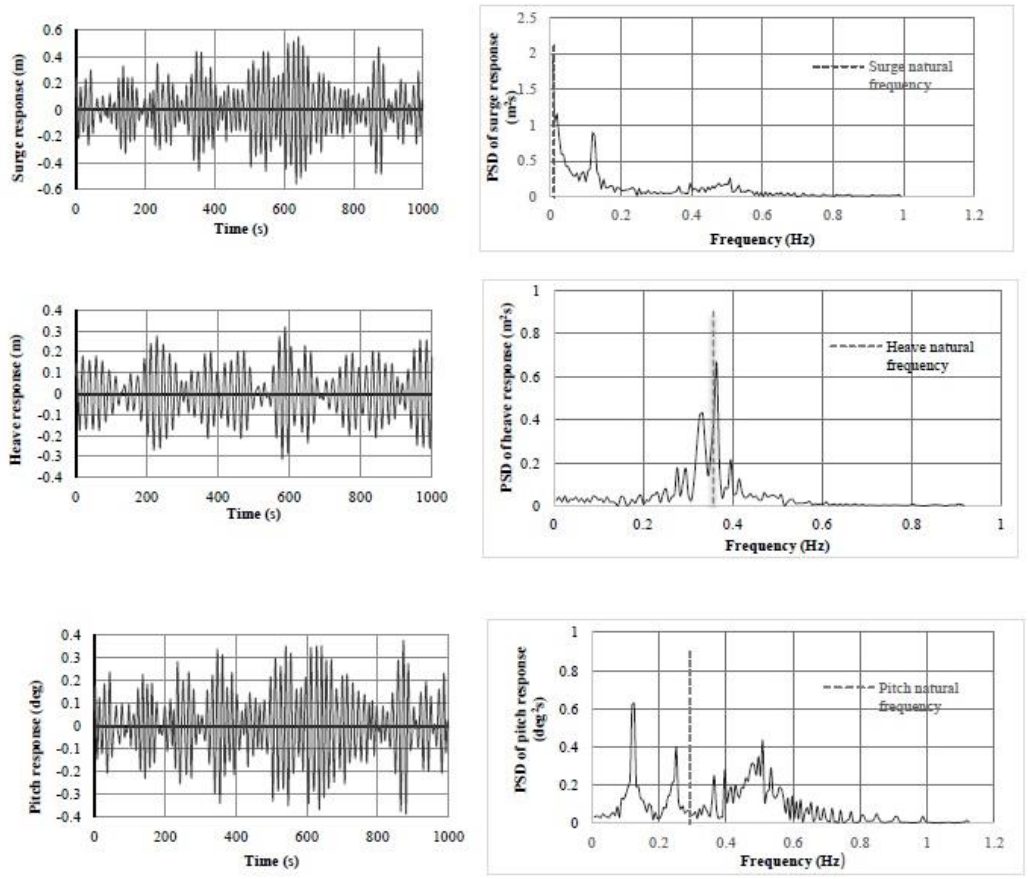

Fig. 8 Response of a buoyant leg group under non-impact waves (Wave set E)

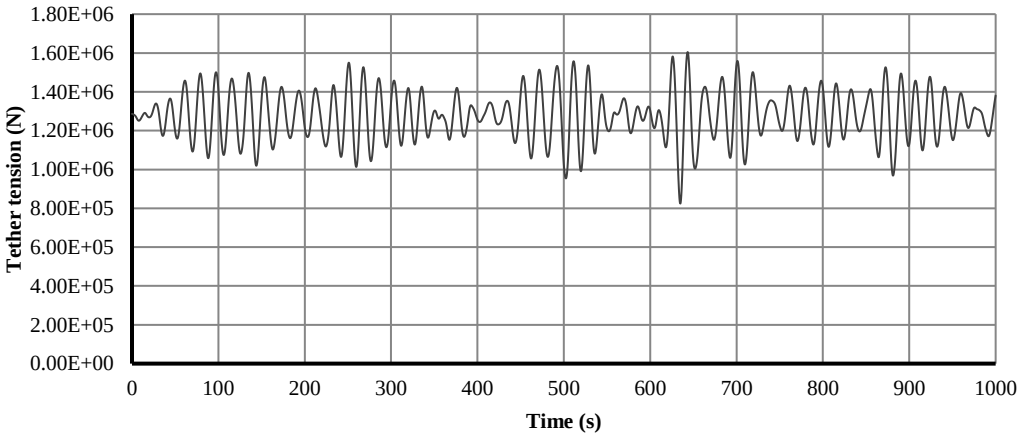

Fig. 9 Tether Tension due to wave E

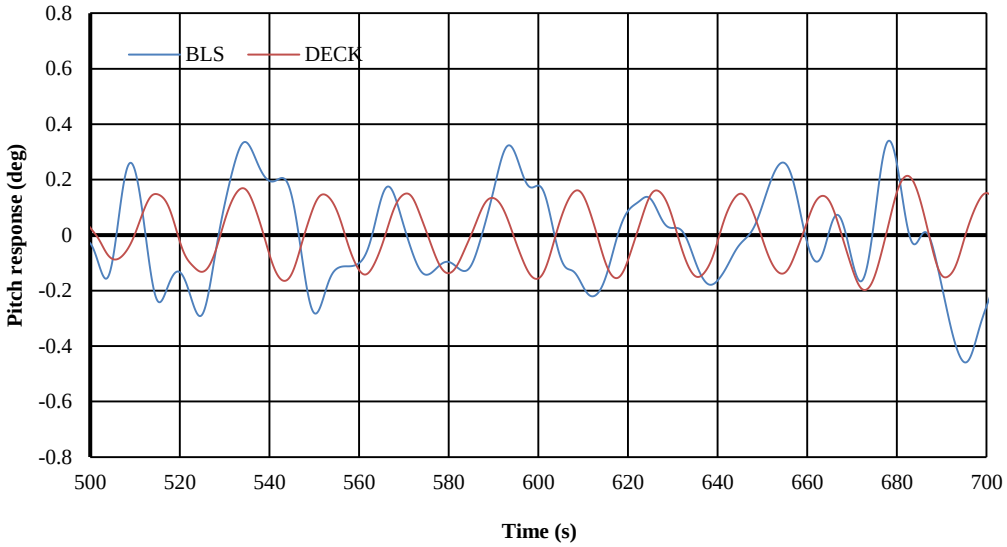

Fig. 10 Comparison of pitch responses under non-impact waves (wave set E)

6. Conclusions

A detailed nonlinear dynamic response of stiffened triceratops under impact and non-impact waves is presented. Two sea states namely: very high and high, with a significant wave height of 9.88 m and 7.62 m are chosen to simulate impact and non-impact waves; their statistical parameters are also verified. It is seen that strong asymmetric waves, resulting in impact waves cause transient response in pitch and heave degrees-of-freedom. Further, weakly asymmetric waves, resulting in non-impact waves cause steady state response. Beat phenomenon is noticed in almost all degrees-of-freedom but values in sway, roll and yaw are considerably low as angle of incidence is zero degrees. Impact waves cause response in higher frequencies; bursting nature of pitch response, occurring closer to 495 s is a clear manifestation of the effect of impact waves on buoyant legs. Impact waves also cause dynamic tether tension variations but maximum amplitude of tether tension variation is only about 2.5% of that of the initial pretension. Non-impact waves cause response similar to that of a beating phenomenon in all active degrees-of-freedom, which otherwise would not be present under normal loading. Power spectral density plots show energy content of response for a wide bandwidth of frequencies, indicating an alarming behaviour apart from being highly nonlinear. Heave, being one of the stiff degrees-of-freedom is triggered under non-impact waves, which resulted in tether tension variation under non-impact waves as well. While stretching modifications of sea surface elevation is done using Chakrabarthi's modification, second-order sum frequency wave diffraction effects are neglected in the springing analysis; this is one of the important limitations of the present study.

Results of numerical studies confirm that springing response affects the deck in significant proportion in comparison to that of the ringing response. Presence of ball joints does not allow transfer of rotational responses from legs to the deck, resulting in safe operability. Reduced deck

response aids functional requirements of triceratops even under impact and non-impact waves. Stiffened group of buoyant legs enable a monolithic behaviour, enhancing stiffness in vertical plane.

References

Capanoglu, C.C., Shaver, C.B, Hirayama, H. and Sao, K. (2002), "Comparison of model test results and analytical motion analyses for a buoyant leg structure", *Proceedings of the 12th Int. Offshore and Polar Eng. Conf*., May 25-31, Kitakyushu, Japan.

Chandrasekaran, S., Bhaskar, K. and Hashim, M. (2010a), "Experimental study on dynamic response behavior of multi-legged articulated tower", *Proceedings of the 29th Int. Conf. on Ocean, Offshore and Arctic Engg*, 6-11th June, Shanghai, China.

Chandrasekaran, S., Chandak, N.R. and Gupta, A. (2006), "Stability analysis of TLP tethers", *Ocean Eng.*, **33**(3), 471-482.

Chandrasekaran, S., Gaurav, G., Giorgio, S. and Salvatore, M. (2011), "Springing and ringing response of Triangular TLPs", *Int. Shipbuild. Progress*, **58**(2-3), 141-163.

Chandrasekaran, S., Gaurav and Jain, A.K. (2010b), "Ringing response of offshore compliant structures", *Int. J. Ocean Climate Syst.*, **1**(3-4), 133-144.

Chandrasekaran, S., Jain, A.K. and Madhuri, S. (2013), "Aerodynamic response of offshore triceratops", *Ships Offshore Struct.*, **8**(2), 123-140.

Chandrasekaran, S. and Jain, A.K. (2016), *Ocean structures: Construction, Materials and Operations*, CRC Press, Florida, ISBN: 978-14-987-9742-9.

Chandrasekaran, S and Nannaware, M. (2013), "Response analyses of offshore triceratops to seismic activities", *Ships Offshore Struct*., **9**(6), 633-642.

Chandrasekaran, S., Madhuri, S., Jain, A.K. and Gaurav. (2010c), "Dynamic response of offshore triceratops under environmental loads", *Proceedings of the Int. Conf. of Marine Tech*., 11-12 Dec, Dhaka, Bangladesh.

Chandrasekaran, S. and Madhuri, S. (2012a), "Free vibration response of offshore triceratops: Experimental and analytical investigations", *Proceedings of the 3rd Asian Conf. on Mech. of Functional Materials and Structures (ACFMS)*, 8-9 Dec, Delhi.

Chandrasekaran, S. and Madhuri, S. (2012b), "Stability studies on offshore triceratops", Proc. Int. Conf. Tech. of Sea, Indian Maritime University, *Vishakapatnam*, 1(10), 398-404.

Chandrasekaran, S. and Madhuri, S. (2015), "Dynamic response of offshore triceratops: Numerical and Experimental investigations", *Ocean Eng.*, **109**(15), 401-409.

Chandrasekaran, S. and Madhuri, S. (2012), "Stability studies on offshore triceratops", *Int. J. Res. Development*, **1**(10), 398-404.

Chandrasekaran, S. and Mayank, S. (2017), "Dynamic analyses of stiffened triceratops under regular waves: experimental investigations", *Ships Offshore Struct.*, **12**(5), 697-705.

Chandrasekaran, S. (2016), *Offshore structural engineering: Reliability and Risk Assessment,* CRC Press, Florida, ISBN: 978-14-987-6519-0.

Chandrasekaran, S. (2015a), *Advanced Marine structures*, CRC Press, Florida, ISBN 9781498739689.

Chandrasekaran, S. (2014), *Advanced Theory on Offshore Plant FEED Engineering*, Changwon National University Press, Republic of South Korea, pp. 237, ISBN:978-89-969792-8-9.

Chandrasekaran, S. (2015b), *Dynamic analysis and design of ocean structures*, Springer, INDIA, ISBN: 978-81-322-2276-7.

Halkyard, J.E., Paulling, J.R., Davies, R.L. and Glanville, R.S. (1991), "Tension buoyant tower: A design for deep water", *Proceedings of the Offshore Tech. Conf*., May 6-9, Houston, TX.

Isherwood, R.M. (1987), "A revised parameterization of the JONSWAP spectrum", Tech. Note, *Appl. Ocean Res.*, **9**(1), 47-50.

Jeffreys, E.R. and Rainey, R.C. (1994), "Slender body models of TLP and GBS ringing", *Proceedings of the Int. Conf. on Behaviour of Offshore Struc*., Massachusetts, USA.

Kim, C.H., Randall, R.E., Boo, S.Y. and Krafft, M.J. (1992), "Kinematics of 2-D transient water waves using laser Doppler anemometry", *J. Waterw. Port, C -ASCE*., **118**(2), 147-165.
Kim, C.H., Xu, Y. and Zou, J. (1998), "Impact and nonimpact on vertical truncated cylinder due to strong and weak asymmetric wave", *Oceanographic Lit. Rev*., **1**(45), 174.
Kim, C.H., Xu, Y. and Zou, J. (1997), "Impact and nonimpact on vertical truncated cylinder due to strong and weak asymmetric waves", *Int. J. Offshore Polar*., **7**(3).
Kim, C.H. (2009), "Nonlinear response of offshore structures to high seas", *Int. J. Offshore Polar*., **19**(1), 1-7.
Longuet-Higgins, M.S. and Cokelet, E.D. (1976), "The deformation of steep surface waves on water: Numerical method of computation", *P. Roy. Soc. London A: Math. Phy*., The Royal Society, 1-26.
Murert, J., Flugstad, P., Greiner, B., D'Souza, R. and Solber, I.C. (1996), "The three-column TLP: A cost efficient deepwater production and drilling platform", *Proceedings of the Offshore Tech. Conf.*, 6-9 May, Houston, Texas.
Myrhaug, D. and Kjeldsen, S.P. (1984), "Parametric modelling of joint probability density distributions for steepness and asymmetry in deep water waves", *App. Ocean Res*., **6**(4), 207-220.
Price, W.G. and Bishop, R.E.D. (1974), "*Probabilistic theory of ship dynamics*", Halsted Press.
Shaver, C.B., Capanoglu, C.C. and Serrahn, C.S. (2001), "Buoyant leg structure: Preliminary design, constructed cost and model test results", *Proceedings of the 11th Int. Offshore and Polar Engg. Conf*., 17-22 June, Stavenger, Norway.
Tromans, P., Swan, C. and Masterton, S. (2006), "Nonlinear potential flow forcing ringing of concrete gravity based structures", *Health and Safety Executive*, United Kingdom, HSE Report, pp. 468.
Tucker, M.J., Challenor, P.G. and Carter, D.J.T. (1984), "Numerical simulation of a random sea: a common error and its effect upon wave group statistics", *App. Ocean Res*., **6**(2), 118-122.
White, C.N., Copple, R.W. and Capanoglu, C. (2005), "Triceratops: An effective platform for developing oil and gas fields in deep and ultra deep water", *Proceedings of the 15th Int. Offshore and Polar Engg. Conf*., June 19-24, Busan, South Korea.
Zou, J. and Kim, C.H. (2000), "Generation of strongly asymmetric wave in random seaway", *Proceedings of the 10th Int. Offshore and Polar Engg. Conf*., May 28 - June 2, Seattle, USA.

MK